ELSEVIER

International Journal of Refrigeration 24 (2001) 417–427

REVUE INTERNATIONALE DU FROID
INTERNATIONAL JOURNAL OF
refrigeration

www.elsevier.com/locate/ijrefrig

Experimental study on the performance of an inverter heat pump with a bypass orifice

Jongmin Choi [a], Yongchan Kim [a,*], Jongyeop Kim [b]

[a] *Department of Mechanical Engineering, Korea University, Seoul, South Korea*
[b] *Samsung Electronics, Suwon, South Korea*

Received 15 September 1998; received in revised form 15 September 1999; accepted 17 March 2000

Abstract

An economical, fixed geometry, bypass orifice was invented to control more precisely the refrigerant flow in an inverter heat pump system. Flow characteristics of the bypass orifice were investigated as a function of orifice geometry and operating conditions. Experimental results of bypass orifices were compared with those of capillary tubes. The bypass orifice showed the best flow trend as a function of frequency: the flow slope of the bypass orifice with respect to frequency was the highest among the orifice, capillary, and bypass orifice. The performance of an inverter heat pump with a bypass orifice and then a capillary tube was measured with a variation of frequency in the psychrometric calorimeter. It was observed that the performance of the inverter heat pump was enhanced with the application of the bypass orifice in the system instead of a capillary tube. The improvement of COP in an inverter heat pump with a bypass orifice versus the capillary tube was prevalent at the low frequency region.

Keywords: Air conditioning; Heat pump; Compressor; Speed; Variation; Valve; Design – optimization

Etude expérimentale sur la performance d'une pompe à chaleur à variation de vitesse munie d'un orifice de dérivation

Résumé

Les auteurs ont développé un orifice de dérivation afin de réguler l'écoulement du frigorigène dans un système de pompe à chaleur à variation de vitesse. Les caractéristiques d'écoulement de l'orifice de dérivation ont été étudiées en fonction de la géométrie de l'orifice et des conditions de fonctionnement. On a comparé les résultats expérimentaux avec ceux des capillaires. L'orifice de dérivation possède le meilleur profil d'écoulement en fonction de la fréquence : la courbe de l'écoulement à travers l'orifice de dérivation en fonction de la fréquence était la meilleure des trois systèmes étudies (orifice, capillaire et orifice de dérivation). Les performances d'une pompe à chaleur munie d'un orifice de dérivation puis d'un capillaire ont été mesurées, avec variation de fréquence, par un calorimètre psychrométrique. On a constaté que la performance de la pompe à chaleur à variation de vitesse a été améliorée lorsqu'on a utilisé un orifice de dérivation au lieu d'un capillaire. L'amélioration du COP d'une pompe à chaleur à variation de vitesse munie d'un orifice de dérivation au lieu d'un capillaire a été importante dans la région des basses vitesses.

Mots clés : Conditionnement d'air ; Pompe à chaleur ; Compresseur ; Vitesse ; Variation ; Détendeur ; Conception – optimisation

* Corresponding author. Tel.: +82-2-3290-3366; fax: +82-2-921-5439.
E-mail address: yongckim@mail.korea.ac.kr (Yongchan Kim).

0140-7007/01/$20.00
PII: S0140-7007(00)00033-5

Nomenclature

A_s	orifice cross-sectional area
C	discharge coefficient for orifice equation
D	orifice diameter
DB	bypass hole diameter
D_{ref}	reference orifice diameter
$EVAP$	normalized downstream pressure
g_c	dimensional gravity constant
LB	position of bypass hole from entrance of bypass orifice
m_s	mass flow rate
P_c	critical pressure
P_{down}	downstream pressure
P_f	adjusted downstream pressure
P_{sat}	upstream liquid saturation pressure
P_{up}	upstream pressure
$SUBC$	normalized subcooling
T_c	critical temperature
T_{sat}	liquid saturation temperature of the upstream fluid
T_{up}	temperature of upstream fluid
β	ratio of orifice diameter to upstream tube diameter
ρ	density
ρ_f	density of liquid

1. Introduction

An inverter heat pump makes the continuous operation of a compressor possible through capacity modulation of the system with respect to the building load utilizing frequency control of the compressor. It also provides several advantages in energy conservation, capacity control and comfort of the indoor environment over the constant speed heat pump [1–5]. In association with an inverter heat pump, the following several topics have been vigorously studied [4–7]: brushless direct current (BLDC) motor, scroll compressor, oil recovery at low temperature heating conditions, performance characteristics and design modification of the system with the application of the HCFC-alternatives, and development of an expansion device suitable for inverter heat pump operation.

The capillary tube, which is suitable for systems of small capacities and advantageous in cost and reliability, is being widely used as the expansion device in the inverter heat pump in Korea. However, in applying a capillary tube to an inverter heat pump system, it is impossible to establish an optimum cycle at all frequencies. Performance degradation of an inverter heat pump system with a capillary tube was obviously observed at low frequencies [8].

Recently, an orifice expansion device has been widely applied to heat pump systems. Most of the previous research associated with the orifice were focused on the rigid orifice suitable for a constant speed heat pump [9–13]. Several researchers conducted experimentation and modeling work to provide a tool for the optimization of orifice design [8–13]. Drucker [14] invented a flexible orifice by modifying both the structure and material of the orifice which was suitable for operation in the heat pump cycle. Flexible material was used and the flow rate of refrigerant was controlled by varying the shape of the orifice corresponding to the downstream and upstream pressures of the orifice. However, the flexible orifice has disadvantages such as complexities in structure and problems in reliability of the flexible material.

In this study, a bypass orifice expansion device simple in structure was designed by modifying the orifice (called the straight orifice) [15]. The basic characteristics of the bypass orifice were measured as a function of operating conditions and orifice geometry in the experimental setup for expansion devices. Test results were compared with those for the capillary tube and the straight orifice. The flow model for bypass orifices was developed from the results of characterization tests. Based on the preliminary tests, the best configuration of a bypass orifice was selected and the possibility of its application in the system was investigated. The performance of the inverter heat pump with the bypass orifice as a function of operational frequency was compared to that of the system having the capillary tube.

2. Experimental setup and test procedure

As shown in Fig. 1, the experimental apparatus for the measurement of basic characteristics of bypass orifices was designed to allow for easy control of each of the operating parameters such as entrance subcooling, condensing and evaporating pressure. The mass flow rate of the refrigerant entering the test section was controlled by varying the rotational speed of the liquid pump. The degree of subcooling of the refrigerant entering the test section was regulated by controlling the temperature and the mass flow rate passing through the water heated evaporation heat exchanger. The exit pressure of the test section was set by both the temperature and the mass flow rate of the water/glycol solution in the condensation heat exchanger.

Fig. 2 shows the test section of the bypass orifice. The bypass orifice designed in the present study was tapered

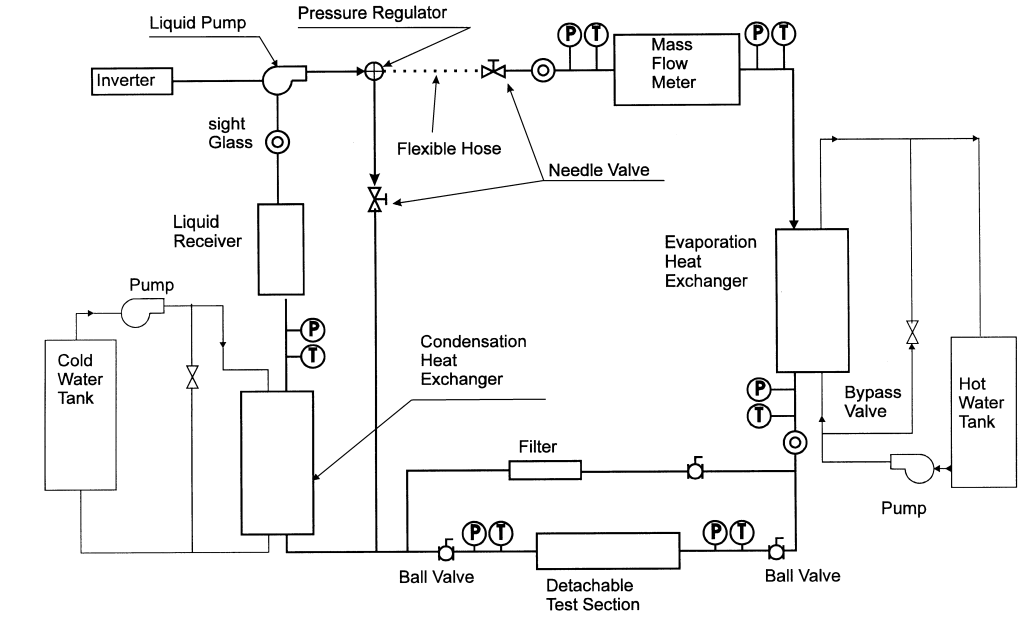

Fig. 1. Schematic diagram of the bypass orifice test setup.

Fig. 1. Schéma de la pompe à chaleur munie d'un orifice de dérivation.

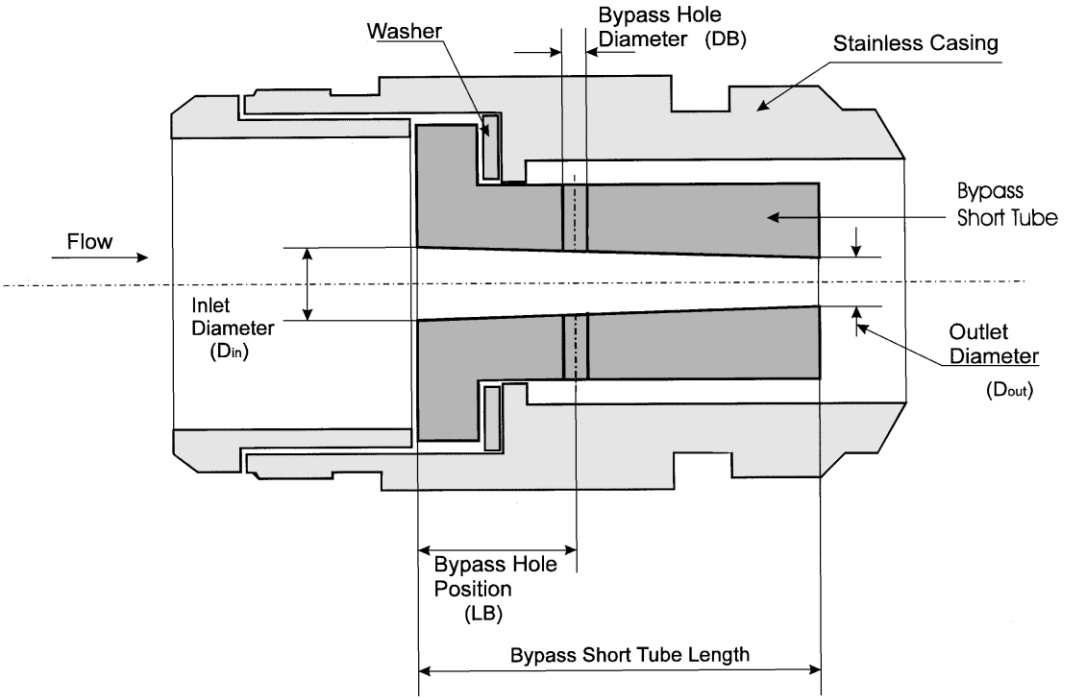

Fig. 2. Test section of a bypass orifice.

Fig. 2. Section à essai de l'orifice de dérivation.

toward the flow direction and had two bypass holes in the middle of the orifice. All the other configurations are identical to the straight orifice that has been widely used in the air conditioning system as an expansion device [9–13].

A schematic diagram of the experimental setup for testing the inverter heat pump with the bypass orifice or the capillary tube is shown in Fig. 3. It was composed of indoor and outdoor rooms. The temperature and humidity of each room were controlled by an air handling unit. The capacity of the heat pump was measured in an air flow chamber using an air-enthalpy method. The dry bulb and wet bulb temperature of the sampling air at the inlet and outlet of the indoor unit were precisely monitored in the air flow chamber. Mass flow rate of air flowing through the indoor unit was calculated by measuring the differential pressure between the inlet and outlet of the nozzle, absolute pressure, nozzle exit temperature, and humidity at the nozzle.

The test unit was a split type inverter heat pump with a rated cooling capacity of 4141 W (3550 kcal/h). It used a single rotary compressor. The indoor unit included a finned-tube heat exchanger with a three path structure of two rows and 14 stages. The outdoor heat exchanger was composed of a two path structure of two rows and 24 stages. The capillary tube and the bypass orifice were used as the expansion devices. Each instrument was installed to obtain data satisfying ASHRAE Standard 116 [16] and ASHRAE Standard 37 [17].

The performance of the inverter heat pump using R-22 was measured at 34, 59 and 72 Hz with the ASHRAE test condition "A" (indoor condition: 27°Cdb, 19.5°Cwb, outdoor condition: 35°Cdb, 24°Cwb). The optimum charge amount into the system for each expansion device was experimentally determined by selecting the value when the maximum COP was obtained with a variation of the refrigerant charge at the rated frequency (59 Hz) and ASHRAE test condition "A".

Each sensor was calibrated to reduce experimental uncertainties and was connected to the data logger. Table 1 represents the accuracy and tolerance of each sensor for measuring data. The uncertainty of the cooling capacity and COP estimated by the single-sample analysis was approximately 2.6%.

3. Results and discussion

Since the inverter heat pump is capable of covering a wide range in capacity corresponding to building load throughout the year, the wide range of refrigerant flow

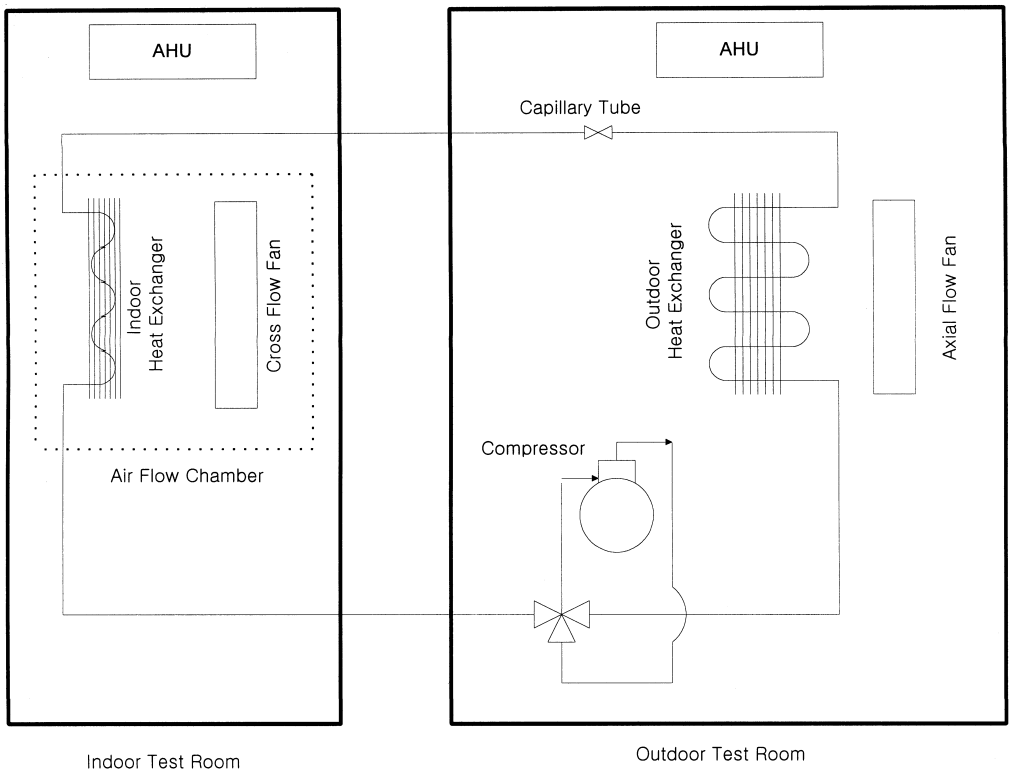

Fig. 3. Schematic diagram of psychrometric calorimeter.

Fig. 3. Schéma du calorimètre psychrométrique.

Table 1
Accuracy and tolerance of the sensors
Tableau 1
Précision et tolérance des capteurs

	Sensor	Accuracy	Tolerance	Full scale	Model
Orifice test setup					
	Temperature	±0.2°C	±0.2°C	–	Thermocouple T-type
	Pressure transducer	±0.2% of full scale	±0.2% of full scale	3447 kPa	Model:Setra C206
	Mass flow meter (Coriolis meter)	±0.2% of full scale	±0.2% of full scale	5 kg/min	Model:Micro Motion D012S-SS-200
Psychrometric calorimeter					
	Temperature	±0.05°C	DB WB ±0.2°C ± 0.15°C	–	RTD(Pt 100 Ω)
	Atmospheric pressure	±0.15% of full scale	±0.15% of full scale	101 kPa	Model:KGI TP-6001
	Differential pressure	±0.4% of full scale	±0.4% of full scale	80 mm H_2O	Model:Rosemount 1151
	Power meter	±0.01% of full scale	±0.5% of reading	20 kW	Model:Yokogawa WT1030
	Electronic balance	±0.5 g	–	41 kg	Model:AND HP-40K
Data acquisition unit		–	–	–	Model:DA100 Yokogawa

regulation is required as a function of frequency of the compressor. Even though a capillary tube is selected to have the best performance at the rated frequency, an inverter heat pump with a capillary tube is not able to represent optimal performance at both low and high frequency levels because it is a constant flow area expansion device. Therefore, an economical expansion device which allows a large variation in mass flow rate with a change in frequency compared to a capillary tube is in demand in order to enhance the performance of an inverter heat pump.

For optimal operation of an inverter heat pump at all frequency levels, a variable area expansion device such as electronic expansion valve (EEV) and thermostatic expansion valve (TXV) would be preferable. However, the structure is more complex and the cost is higher than a constant area expansion device. Therefore, in the present study, the bypass orifice was designed by modifying the straight orifice. The performances of the inverter heat pump with both the bypass orifice and capillary tube were measured and compared.

Comparing the COP of the system with each capillary tube which has different lengths with the same diameter at the rated frequency (59Hz) and ASHRAE test condition "A", the base capillary tube which showed the best performance among them was selected. The base capillary tube has diameter of 1.7 mm and length of 800 mm.

3.1. Flow characteristics of a bypass orifice

Based on the tests results of the inverter heat pump with the base capillary tube and other capillary tubes showing maximum performance at each frequency level, the following results were obtained. For a low frequency level, the inverter heat pump showed the maximum performance when the mass flow rate was adequately decreased by increasing the capillary tube length as compared with the base capillary tube. Whereas for a high frequency level, it represented the maximum performance when the mass flow rate was increased by decreasing the capillary tube length as compared with the base capillary tube. Therefore, to improve the performance of the system at all frequency levels, the slope of mass flow rate increment as a function of frequency must be greater than that of the capillary tube.

Fig. 4 shows the mass flow rate through the bypass orifice as a function of the upstream (condensing) pressure for different degrees of subcooling. As the upstream pressure increases with a constant degree of entrance subcooling, the entrance pressure drop and internal pressure of the orifice increase [8–13]. The former increases the major mass flow rate passing through the main orifice, and the latter increases the bypass mass flow rate passing through the bypass hole.

Fig. 5 shows the effects of the inlet subcooling on the mass flow rate. As the level of subcooling increases, the density and entrance pressure drop increase, but the internal pressure of the orifice decreases [8–13]. The former tends to increase the major mass flow rate, but the latter decreases the bypass mass flow rate. The increase of the major mass flow rate was larger than the decrease of the bypass mass flow rate as the inlet subcooling increased. Thus, the total flow rate through main and bypass orifice increased with the increase of the degree of inlet subcooling.

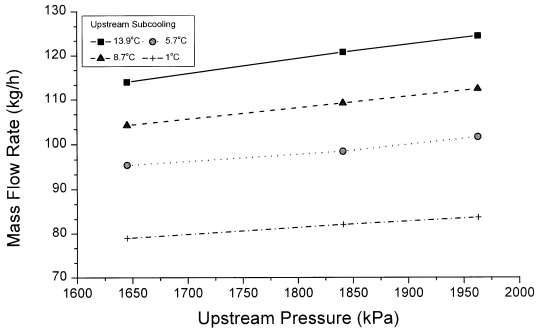

Fig. 4. Flow dependency on upstream pressure for the bypass orifice with $L=15$ mm, $D_{in}=1.38$ mm, $D_{out}=0.92$ mm, $LB=7.92$ mm, and $DB=0.56$ mm.

Fig. 4. Ecoulement en fonction de la pression en amont pour l'orifice de déviation où $L=15$ mm, $D_{in}=1,38$ mm, $D_{out}=0,92$ mm, $LB=7,92$ mm, et $DB=0,56$ mm.

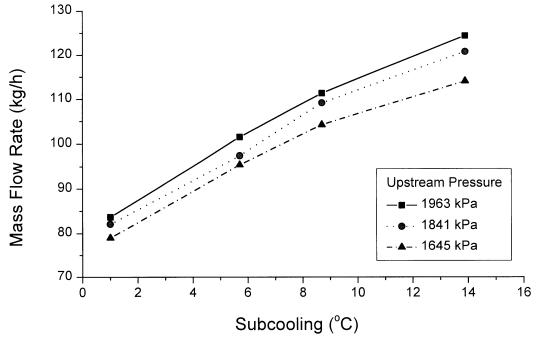

Fig. 5. Flow dependency on upstream subcooling for the bypass orifice with $L=15$ mm, $D_{in}=1.38$ mm, $D_{out}=0.92$ mm, $LB=7.92$ mm, and $DB=0.56$ mm.

Fig. 5. Ecoulement en fonction du sous-refroidissement en amont pour l'orifice de déviation où $L=15$ mm, $D_{in}=1,38$ mm, $D_{out}=0,92$ mm, $LB=7,92$ mm, et $DB=0,56$ mm.

Fig. 6 shows the effects of downstream(evaporating) pressure on the mass flow rate for three different upstream pressures. For the downstream pressure below the liquid saturation pressure corresponding to the upstream temperature, the mass flow rate became relatively independent of the downstream pressure. Choked flow was observed in the bypass orifice and these trends were identical to that of capillary tubes and straight orifices [9].

Fig. 7 shows the effects of bypass hole position on the mass flow rate for three different upstream pressures. As the position of the bypass hole moves toward the exit of the bypass orifice, the internal pressure of the bypass orifice decreases [8–13]. Therefore, the pressure at the inlet of the bypass hole decreases as the location of the

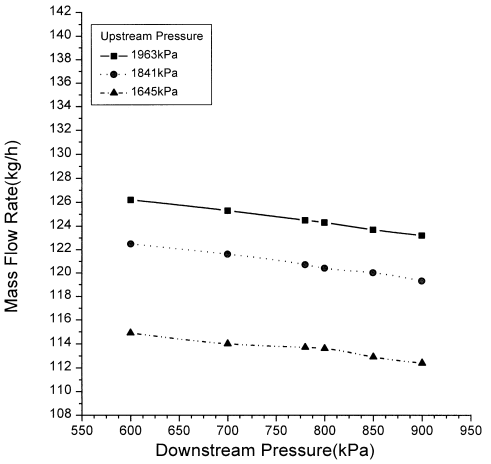

Fig. 6. Flow dependency on downstream pressure for the bypass orifice with $L=15$ mm, $D_{in}=1.38$ mm, $D_{out}=0.92$ mm, $LB=7.92$ mm, and $DB=0.56$ mm.

Fig. 6. Ecoulement en fonction de la pression en aval pour l'orifice de déviation où $L=15$ mm, $D_{in}=1,38$ mm, $D_{out}=0,92$ mm $LB=7,92$ mm, et $DB=0,56$ mm.

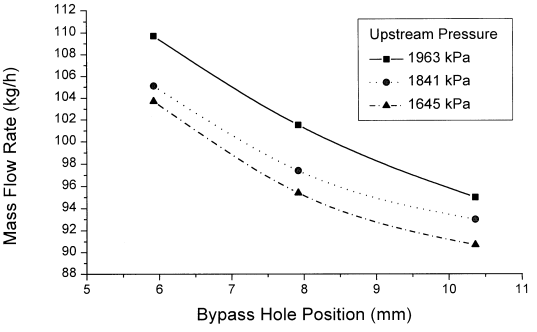

Fig. 7. Flow dependency on bypass hole position for bypass orifice with $L=15$ mm, $D_{in}=1.38$, $D_{out}=0.92$ mm, $LB=7.92$ mm, and $DB=0.56$ mm.

Fig. 7. Ecoulement en fonction de l'emplacement de l'orifice où $L=15$ mm, $D_{in}=1,38$ mm, $D_{out}=0,92$ mm $LB=7,92$ mm, et $DB=0,56$ mm.

bypass hole is moved to the exit of the bypass orifice. As a result, the mass flow rate through the bypass hole decreases. The slope of the mass flow rate of the bypass orifice with a variation of frequency can be altered by moving the location of the bypass hole.

Fig. 8 shows the effects of frequency on mass flow rate for the capillary tube, straight orifice, and bypass orifice. The data for the capillary tube was obtained by utilizing the existing flow model [8]. The others were the measured data from experimentation. The operating

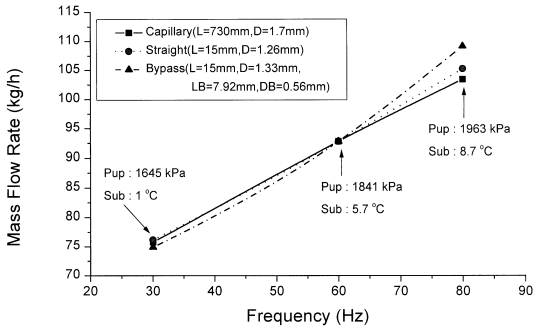

Fig. 8. Comparison of flow dependency on frequency.

Fig. 8. Ecoulement en fonction de la fréquence.

conditions at each frequency were selected based on the results of the performance test of the inverter heat pump with the capillary tube.

When the mass flow rate at the rated frequency was identically set for all of the expansion devices to provide the reference point, the slope of mass flow rate for the bypass orifice as a function of frequency was greater than that of the straight orifice or the capillary tube. The mass flow rate of the capillary tube linearly increases [9] corresponding to the inlet pressure and subcooling, but increases nonlinearly with respect to subcooling in the straight orifice [8–13]. Therefore, the slope of the mass flow rate of the straight orifice as to the frequency was greater than that of the capillary tube.

The mass flow rate of the bypass orifice as a function of the inlet pressure and subcooling was similar to that of the straight orifice. However, the bypass orifice had a bypass hole, and the main hole was tapered toward flow direction. If the entrance pressure of the bypass orifice is increased, the flow rate through bypass hole increased due to two reasons. First, the pressure at the inlet of the bypass hole was raised because internal pressure of the bypass orifice increased. Second, the degree of subcooling at the inlet of the bypass hole increased because the flashing point moved to the exit of the bypass orifice. Therefore the mass flow rate of the bypass orifice was also affected by the location of flashing point and internal pressure.

3.2. Mass flow model of a bypass orifice

The mass flow model of the bypass orifice was developed to predict the mass flow rate at given flow conditions and orifice geometry. This model was developed based on the form of Aaron and Domanski's model [9] and Kim's model [10].

The single-phase orifice equation derived from the continuity and energy conservation equations is given as follows [9,10],

$$\dot{m}_s = CA_s\sqrt{2\rho g_c(P_{up} - P_{down})/(1-\beta^4)} \quad (1)$$

where β is the ratio of orifice diameter to upstream tube diameter.

The assumptions, control volume, and governing equations applied in the straight orifice model must be modified in its application to the bypass orifice. Fig. 9 shows the control volume modified for the bypass orifice. Since the effect of the downstream pressure on the mass flow rate is negligible in the choking conditions, the boundary surface of the downstream was moved to an arbitrary pressure surface in front of the choking point. If the bypass orifice downstream pressure is below the saturation pressure corresponding to the inlet temperature, the internal pressure of the bypass orifice is also below the saturation pressure. Despite the pressure at the inlet section being lower than the saturation point, the flow in this region is in the superheated liquid state, or the so-called metastable state. In the metastable liquid state, the change of temperature is minor due to the coincidence of the constant temperature with the pressure drop line along the flow direction. Temperature in the new control volume shown in Fig. 9 was nearly constant and density variation of liquid was also negligible because there was no evaporation. Therefore, the assumptions of incompressible flow and isothermal process were satisfied.

In order to satisfy flow characteristics and conditions of the flow, the governing equation was modified as follows. The term of β^4 was neglected in Eq. (1) because β was small, ranging between 0.13 and 0.15. The orifice constant, C, was fixed at 1. In order to satisfy the downstream pressure of the control volume, downstream pressure P_{down} was replaced with P_f which was the pressure before evaporation. P_f was composed of dimensionless parameters, which were functions of inlet pressure, inlet subcooling, downstream pressure and inlet diameter of the bypass orifice. The coefficients of each term of the flow model were determined by nonlinear regression with the experimental data. The value of the coefficients of P_f is listed in Table 2.

$$\dot{m}_s = A_s\sqrt{2\rho_f g_c(P_{up} - P_f)} \quad (2)$$

$$P_f = P_{sat}[a_1 + a_2(P_{up}/P_c)^{a_3}(D/D_{ref})^{a_4}SUBC^{a_5} + a_6(P_{up}/P_c)^{a_7} + a_8(EXP(a_9(D/D_{ref})) + a_{10}EVAP] \quad (3)$$

where $SUBC = (T_{sat} - T_{up})/T_c$

$EVAP = (P_c - P_{down})/P_c$

The maximum difference between the measured data and the model's prediction was within a ±5% margin. The application of the flow model has a limited range bounded by the test range of the experimental data as given in Table 3.

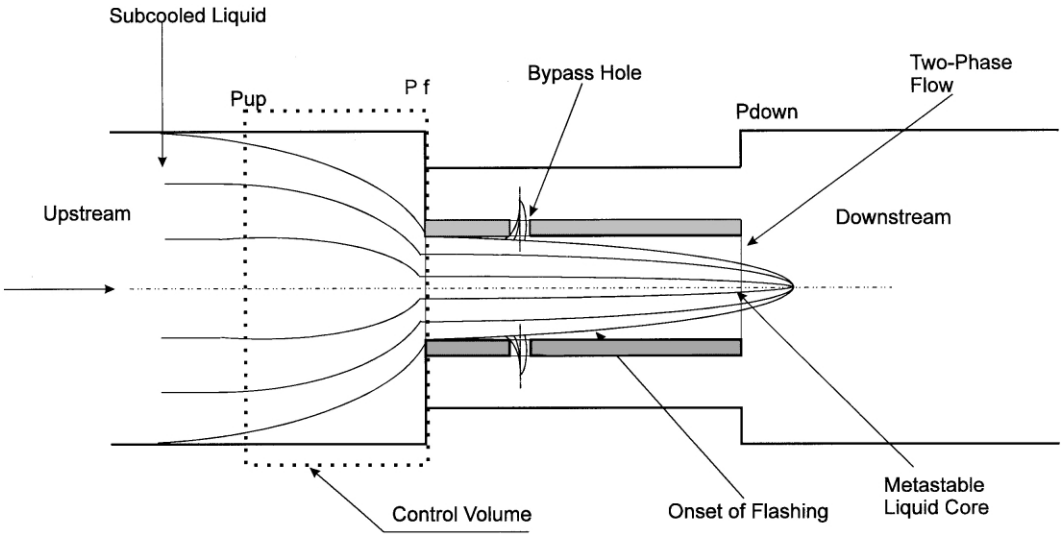

Fig. 9. Control volume of the flow model.

Fig. 9. Zone de contrôle de débit du modèle d'écoulement.

Table 2
Coefficients of correction factors in the flow model

Tableau 2
Coefficients des facteurs de correction dans le modèle d'écoulement

Equations	Coefficients	HCFC-22
Eq. (2)	a_1	0.02706
	a_2	11.35237
	a_3	−0.68358
	a_4	1.17439
	a_5	1.31613
	a_6	0.11144
	a_7	−0.3044
	a_8	0.67779
	a_9	0.0829
	a_{10}	0.04805
	P_c	4973.8 kPa
	T_c	369.3 K
	g_c	1.2960×10^{10}

Table 3
Limitation on the application of the flow model

Tableau 3
Limite d'application du modèle d'écoulement

HCFC-22	Parameter	Minimum	Maximum
Geometries	Length	15 (mm) fixed	
	Inlet diameter	1.33 (mm)	1.43 (mm)
	DB	0.5 (mm) fixed	
	LB	8 (mm) fixed	
	Tapering angle	1° fixed	
Operating conditions	P_{up}	1645 (kPa)	1963 (kPa)
	P_{down}	600 (kPa)	900 (kPa)
	Subcooling	1°C	13.9°C

3.3. Application of a bypass orifice to the system

Based on the results of characterization tests and preliminary tests, the optimum bypass orifice for the heat pump was selected. Table 4 shows the results of the performance test of the inverter heat pump with the capillary tube and the bypass orifice. The optimum capillary tube at each frequency was determined by comparing the performance of the inverter heat pump with a variation in capillary tube length. The performance with the optimum capillary would be the maximum performance at each frequency level.

Employing the bypass orifice to the inverter heat pump, the evaporating pressure slightly decreased at the frequency of 34 Hz, but the condensing pressure, superheat and subcooling increased compared to those of the base capillary tube applications (Figs. 10 and 11). The refrigerant flow rate of the system with the bypass orifice was less than that of the base capillary tube at a low frequency level (Fig. 12). However, the enthalpy difference between the inlet and outlet of the evaporator increased because of the increase of inlet subcooling and superheat. As a result, the cooling capacity of the system with the bypass orifice was enhanced compared to the system utilizing the base capillary tube at low

Table 4
Comparison of performance of an inverter heat pump with a capillary tube and bypass orifice

Tableau 4
Comparaison de la performance d'une pompe à chaleur à vitesse variable muni d'un capillaire et d'un orifice de dérivation

		Frequency (Hz)		
		34	59	72
Capacity (W)				
	Optimum capillary	2716.9	3969.8	4552.8
	Capillary (base)	2559.1	3969.8	4355.2
	Bypass orifice	2659.9	3928.3	4310.9
Power(W)				
	Optimum capillary	940.6	1528.3	1934.6
	Capillary (base)	969.4	1528.3	1898.9
	Bypass orifice	933.3	1492.4	1858.5
COP				
	Optimum capillary	2.89	2.59	2.35
	Capillary (base)	2.64	2.59	2.29
	Bypass orifice	2.85	2.63	2.32

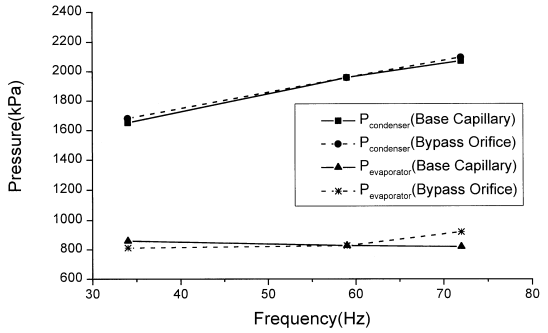

Fig. 10. Variation of condensing and evaporating pressure as a function of frequency.

Fig. 10. Variation des pressions de condensation et d'évaporation en fonction de la fréquence.

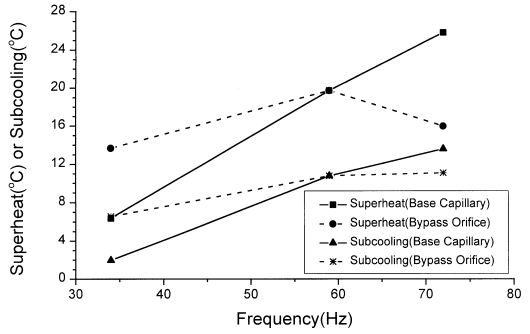

Fig. 11. Superheat and subcooling as a function of frequency.

Fig. 11. Surchauffe et sous-refroidissement en fonction de la fréquence.

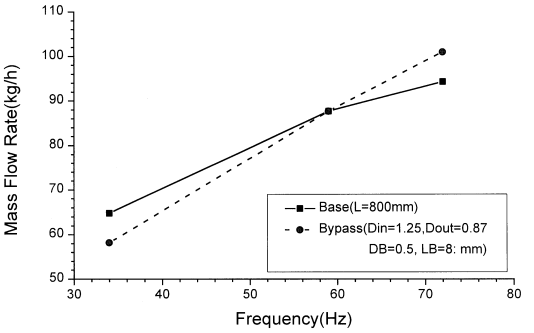

Fig. 12. Variation of mass flow rate as a function of frequency.

Fig. 12. Variation du flux massique en fonction de la fréquence.

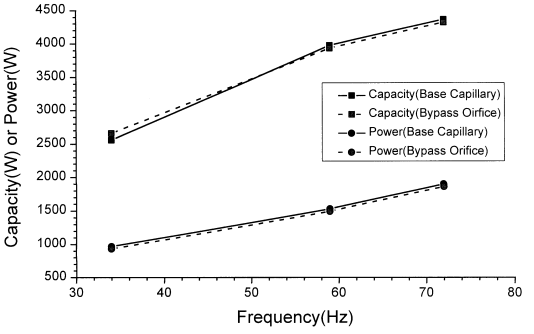

Fig. 13. Variation of capacity and power input as a function of frequency.

Fig. 13. Variation de la puissance et de la consommation d'énergie en fonction de la fréquence.

frequency level. When the bypass orifice was replaced with the capillary tube at the frequency of 34 Hz, the power consumption of the system decreased from 969.3 W to 933.3 W by 3.7% and cooling capacity increased from 2559.1 W to 2659.9 W by 3.9%. Since the capillary tube was not able to cover a wide range of flow rates, the mass flow rate at a low frequency level was not adjusted to the required value. Generally, at a low frequency level, a lower flow rate is required. Consequently, the COP of the system with the bypass orifice was enhanced by 7.9% (Figs. 13 and 14).

As the frequency was increased from low to high, cooling capacity and power consumption of the inverter heat pump increased while the COP decreased in both cases of optimum and base capillary tubes (Figs. 13 and 14). Since the condensing pressure, degree of superheat and refrigerant flow rate increased as frequency increased, power consumption of the compressor increased. The cooling capacity also increased because of the increase in refrigerant flow rate and enthalpy difference across

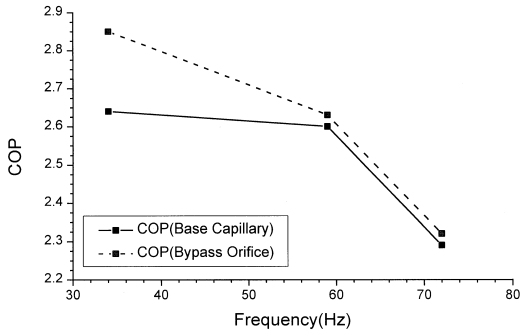

Fig. 14. Variation of COP as a function of frequency.

Fig. 14. Variation du COP en fonction de la fréquence.

the evaporator. However, the increase of power consumption with a rise of frequency was greater than the increase in cooling capacity. As a result, the COP dropped with an increase of frequency.

As the result of applying the bypass orifice to the inverter heat pump, the performance of the system improved at all frequencies compared to the case of applying the capillary tube. Especially, the system performance enhanced considerably at a low frequency level. Since the inverter heat pump used in climates in areas such as Korea is operated mostly at the rated frequency and at a low frequency level, the SEER of the system will be improved by applying a bypass orifice into an inverter heat pump.

4. Conclusions

In the present study, a bypass orifice was designed for its application into an inverter heat pump by modifying the straight orifice. The characteristics of the bypass orifice were measured, and the flow model was developed. The performances of the heat pump with both the bypass orifice and the capillary tube were measured and compared. As a result, the following conclusions were derived.

When the mass flow rate of the bypass orifice was identical to that of the capillary tube and straight orifice at the rated frequency, the bypass orifice showed a lower mass flow rate at a low frequency level due to an increase of flow resistance while it had a higher mass flow rate at a high frequency level due to a decrease of flow resistance compared to that of the capillary tube and the straight orifice. Based on the results of flow characterization tests, a semi-empirical flow model was developed to predict the mass flow rate of bypass orifices with given conditions and orifice geometry. The maximum difference between the measured data and the model's prediction was within ±5%. The improvement of the COP by applying the bypass orifice into the inverter heat pump was approximately 8% at low frequency level compared to the system applying the base capillary tube.

Acknowledgements

This work was supported by the Korea Energy Management Corporation.

References

[1] Choi JM, Kim YC, Kim JY, Bae YD. Experimental study on the performance characteristics of an inverter heat pump with a variation of a capillary tube. In: Proceedings of the SAREK Annual Winter Conference, 1996. p. 227–233.

[2] Benton, R. Heat pump setback: computer prediction and field test verification of energy savings with improved controls. ASHRAE Journal 1982:23–9.

[3] Lorentzen G. Heat pumps — where are improvements possible? An exercise in energy. International J of Refrigeration 1986;9:105–107.

[4] Tassou SA, Marquand CJ, Wilson DR. Comparison of the performance of capacity controlled and conventional on/off controlled heat pumps. Applied Energy 1983; 14:241–56.

[5] Senshu T, Arai A, Oguni K, Harada F. Annual energy-saving effect of capacity-modulated air conditioner equipped with inverter driven scroll compressor. ASHRAE Trans 1985;91(Part 2B):1569–84.

[6] Hayashi M, Nariai S. Development of scroll inverter air conditioners. Refrigeration 1992;67(772):51–7.

[7] Okoma K, Tahata M, Tsuchiyama H, Study of twin rotary compressor for air-conditioner with inverter system. In: Proceeding of the 1990 International Compressor Engineering Conference at Purdue, 1990. p. 541–547.

[8] Kim YC, Choi JM. Comparison of the characteristics of a capillary tube with those of an short tube orifice. In: Proceedings of the SAREK Annual Summer Conference, 1995. p. 242–7.

[9] Aaron AA, Domanski PA. An experimental investigation and modeling of the flow rate of Refrigerant 22 through the short tube restrictor. ASHRAE Transactions 1989; 96(1):729–42.

[10] Kim Y. Two-phase flow of HCFC-22 and HFC-134a through short tube orifices. PhD dissertation, Texas A&M University, 1993.

[11] Kim Y, O'Neal DL. Two-phase flow of R-22 through short-tube orifices. ASHRAE Transactions Vol 1994; 100(1):323–34.

[12] Kim Y, O'Neal DL, Yuan X. Two-phase flow of HFC-134a and CFC-12 through short-tube orifices. ASHRAE Transactions Vol 1994;100(2):582–91.

[13] Kim Y, O'Neal DL. A comparison of critical flow models for estimating two-phase flow of HCFC22 and HFC134a through short tube orifices. Int J of Refrigeration 1995; 18(7):447–55.

[14] Drucker. United States Patent, nos. 5038579, 5080286, 5134860, 1992.
[15] Kim JY, Kim Y. United States Patent, no. 5862676, 1999.
[16] ASHRAE. Method of testing for seasonal efficiency of unitary air-conditioners and heat pumps, ASHRAE Standard ANSI/ASHRAE 116-1983, 1983.
[17] ASHRAE. Method of testing for rating unitary air-conditioning and heat pump equipment. ASHRAE STANDARD 37-1988, 1988.